



Correlation of electrical measurements with moisture content for the diagnosis of preservation levels of neapolitan traditional masonries and the determination of recovery interventions

Veronica Vitiello^{a,*}, Roberto Castelluccio^a, Paola Villoria Sáez^b

^a Department of Civil Building and Environmental Engineering of University of Naples Federico II, Piazzale V. Tecchio 80, 80125 Naples, Italy

^b Grupo de Investigación TEMA, Universidad Politécnica de Madrid. Escuela Técnica Superior de Madrid, Avenida Juan de Herrera 6 28240 Madrid Spain

ARTICLE INFO

Keywords:

Building preservation
Non-destructive diagnosis
Electrical diagnosis
Moisture phenomena
Recovery intervention

ABSTRACT

The humidity phenomena leads to the deterioration of walls' performance. The recovery project relies on prior knowledge of the existing preservation levels. Innovative studies are exploring non-destructive electrical diagnosis methods to determine moisture contents and the correlation with measured electrical parameters. The research presented in this paper modifies the traditional methodological approach and defines a method for measuring the performance levels of wet tuff masonry. This method is based on comparing electrical measurements conducted in the laboratory. The innovative approach allows measurements to be taken without the constraints of probes design and external interference, overcoming limitations of current applications.

1. Introduction

Bibliographic studies have widely demonstrated that the presence of moisture inside traditional walls, together with seriously damaging building elements, represents a high vulnerability factor for their performance preservation [1]. Several degradation phenomena occur because of the interference between porous building materials and the water present in foundation soils, which are rich in salts [2]. UNI EN 772-1 [3] takes into account the influence of the evaporative methods used to dispose of moisture contents by mechanical performance of building materials, estimating a maximum reduction in compressive strength of 20 % when moist stones are subjected to forced evaporation. Numerous studies carried out both on natural stones [4–7] and on bricks [8–10], show that this reduction percentage can be exceeded when building materials are in varying saturated conditions, thus having a significant impact on static safety. Some bibliographic references are summarized in Table 1, where the compressive strengths decrease refers to the values recorded for the materials' dry condition ($S = 0\%$).

Due to the presence of humidity, there is also a reduction in the thermal performance of the building materials, which implies a reduction in the energy efficiency of the masonry built with such building materials. The assessment of the building envelope's transmittance, following indications provided by UNI EN ISO 6946 [16], requires that

building envelope's technical elements comply with certain transmittance limit values. However, in design calculations, thermal transmittance is determined through the use of standard materials' thermal conductivities. Many studies have highlighted a significant discrepancy between the theoretical thermal performance of masonries and the real behaviour detected on-site due to the presence of moisture [17–22]. A preliminary comparative analysis on this discrepancy can be made, assuming that values calculated by software pertain to materials in dry conditions while values directly measured correspond to materials in real exercise conditions. These conditions, influenced by hygro-thermal interaction with the external environment and without any decay phenomena linked to the moisture, can be considered in saturation degrees close to 20 %–30 %.

To bridge this information gap, previous results of this investigations directly measured the increase of thermal conductivity of bricks at different saturation levels [9]. The results demonstrated that, passing from dry ($S = 0\%$) to semi-saturated conditions ($S = 50\%$), thermal conductivity of traditional building materials reaches values that are twice those standard, and it can increase by more than 100 % at the saturated condition ($S = 100\%$). In operational conditions with $S = 20\text{--}30\%$, a loss of thermal properties is recorded especially for more porous materials. A selection of bibliographic references illustrating this thermal behaviour are summarized in Table 2, where the increase in

* Corresponding author.

E-mail addresses: veronica.vitiello@unina.it (V. Vitiello), roberto.castelluccio@unina.it (R. Castelluccio), paola.villoria@upm.es (P.V. Sáez).

Table 1
Compressive strength reduction due to the presence of moisture.

Reference	Compressive strength decrease recorded	Saturation condition	Analysed material	
UNI EN 772-1	20,0%	S = 0,0% after forced evaporation	Masonry's samples	[3]
Vitiello et al, 2020	5,1%	20–30 %	Bricks produced by air hardening	[9]
Vitiello et al, 2020	10,2%		Bricks produced by furnace hardening	[9]
Vitiello et al, 2020	29,2%	50,0%	Bricks produced by air hardening	[9]
Vitiello et al, 2020	13,5%		Bricks produced by furnace hardening	[9]
Vitiello et al, 2022	37,0%		Neapolitan Yellow Tuff	[7]
Franzoni et al, 2015	15,0%		Bricks masonries samples	[8]
Ceroni et al, 2004	27,0%		Yellow Tuff	[6]
Ceroni et al, 2004	42,0%		Grey Tuff	[6]
Vitiello et al, 2020	3,8%	100,0%	Bricks produced by air hardening	[9]
Vitiello et al, 2020	4,6%		Bricks produced by furnace hardening	[9]
Vitiello et al, 2022	45,0%		Neapolitan Yellow Tuff	[7]
Verstrynge et al, 2013	46,7%		ferruginous sandstone	[5]
Franzoni et al, 2015	0,3%		Bricks masonry's samples	[8]
Ceroni et al, 2004	37,0%		Yellow Tuff	[6]
Ceroni et al, 2004	43,0%		Grey Tuff	[6]
Colback & Wild	50,0%		Shale and quartzitic sandstone	[11]
Dyke & Dobereiner	76,0%		Penrith sandstone	[12]
Hawkins & McConnell	22,0%		British sandstone	[4]
Lashkaripour & Ghafoori	97,0%		Oolitic limestone	[13]
Vásárhelyi	76,0%		British sandstone	[14]
Vásárhelyi	66,0%		Miocene limestone	[15]

thermal conductivity pertains to values recorded for materials in dry conditions ($S = 0 \%$).

Acoustic properties of building materials are less affected by the presence of humidity [23]. Additionally, chemical and biological degradation phenomena develop due to the presence of moisture, especially if it originates from humidity ascent. Saline solutions contained in foundation soils, in fact, lead to the formation of ettringite and/or thaumasite due to the reaction between sulphate salts and hydrated calcium silicates or aluminates present in hydraulic lime or lime-pozzolan-based mortars, as well as in Portland cement-based mortars used in past recovery interventions [24,25].

Considering these factors, a thorough diagnosis phase aimed at determining the real preservation level of traditional masonries is considered mandatory before undertaking any recovery intervention

Table 2
Thermal conductivity increase due to the presence of moisture.

Reference	Thermal conductivity increase recorded	Saturation condition	Analysed material	
Vitiello et al, 2020	2,2%	S = 20–30 %	Bricks produced by air hardening	[9]
Vitiello et al, 2020	20,8%		Bricks produced by furnace hardening	[9]
Evangelisti et al, 2015	30,0%	Exercise condition assumed to be close to S = 25–30 %	Natural aggregates concrete	[21]
Evangelisti et al, 2015	35,0%		Expanded clays concrete	[21]
Evangelisti et al, 2015	44,0%		Autoclave concrete	[21]
Evangelisti et al, 2015	37,0%		Volcanic inert concrete	[21]
Marshall et al, 2017	23,2%		Bricks	[22]
Vitiello et al, 2020	46,1%	S = 50 %	Bricks produced by air hardening	[9]
Vitiello et al, 2020	90,9%		Bricks produced by furnace hardening	[9]
Vitiello et al, 2020	113,5%	S = 100 %	Bricks produced by air hardening	[9]
Vitiello et al, 2020	162,3%		Bricks produced by furnace hardening	[9]

[26]. Depending on residual performance, design strategies may vary, ranging from light recovery interventions, about maintenance of walls and finishes, to more substantial interventions that include consolidation or replacement of degraded portions that have permanently lost their original characteristics.

With this in mind, the research presented in this contribution, introduces an innovative method to establish the preservation level of traditional masonries, through the use of non-destructive methods, in order to design recovery interventions on Built Heritage.

1.1. Methods for detecting moisture phenomena

Literature review deepens several diagnosis methods aimed at determining the presence of moisture inside construction materials, basically categorizing them into two classes: destructive methods, which involves extracting samples from the masonry for laboratory tests; non-destructive methods, which can be applied directly on the surface [27]. Destructive methods provide the determination of the quantity of water in the walls. Only two measurement methods have been scientifically recognized by standards: the weight method (or gravimetric), regulated by UNI 11085 [28], which is a direct test measuring the moisture content as a ratio between wet and dry weights of a sample; the calcium carbide method, regulated by UNI 11121 [29], which is an indirect test measuring the moisture content as a result of the chemical reaction between the water contained in the sample and the calcium carbide. Both methods involve extracting samples from the wall for subsequent laboratory tests. Due to this invasive nature, their application is not recommended in buildings with significant historical and artistic value. Another limitation concerns the influence of salts taken during the sampling phase, which may affect the validity of these methods because

their volume interferes with the small samples of a few grams taken for testing [30].

1.2. Non-destructive methods for moisture diagnosis on Cultural Heritage

When dealing with Cultural Heritage, it is necessary to employ non-destructive methods, although they may be less precise in data processing [31]. These methods are often classified as qualitative, since they investigate the presence of water based on variations in building materials' properties [32]. This category includes visual investigation, graphical and photographic survey [31], which help localize decay phenomena and identify portions of the wall in bad preservation conditions. In these investigations, these areas appear in equilibrium with the surroundings, while the wet parts reveal phenomena associated with accelerated decay due to the presence of moisture and salts on the surface of porous building materials.

Among non-destructive methods, techniques such as gamma radiation scanning [33], electrical capacitance tomography [34], electrical impedance spectrometry [35,36], moisture meters [37], infrared thermography [38], optical and videography [39,40], dielectric methods [41], microwave and electrical impedance tomography [42] are included. Only some of them, such as gamma radiation scanning, electrical capacitance tomography, infrared thermography and electrical impedance tomography, provide assessable parameters to describe both the presence of moisture and its distribution within a masonry [27]. One of the most commonly used methods in the field of construction materials is the infrared thermography IRT, which allows for determining the distribution of surface temperatures associated with evaporative phenomena [43,44]. Operating under the assumption that the water inside a masonry affects its ability to transmit heat to the external environment, IRT investigation is often employed for the superficial diagnosis of thermo-hygrometric anomalies [45]. Experimental studies have demonstrated the potential of IRT in interpreting evaporative phenomena based on environmental conditions [43,44]. However, these research results reveal that numerous factors influence surface thermal behaviour. Consequently, to obtain a correct interpretation of thermographic images, a preliminary survey on materials' properties and environmental conditions is necessary [46].

1.3. Electrical methods: Advantages and criticalities

Innovative studies on assessing the moisture content of historic buildings promote non-destructive diagnosis through dielectric and microwave tests in order to achieve semi-quantitative results [30,34,46]. Dielectric methods measure the change in the dielectric constant of building materials associated with the moisture content, given that the permittivity of water is significantly higher than that of test samples. Microwave methods, on the other hand, measure the attenuation of microwaves passing through the wet material [27]. Challenges arise in these methods when sensors do not adhere properly to the wall, affecting the accuracy of measurements [41,47,48]. To address this issue, some researchers have explored the use of passive sensors fabricated in Low Temperature Co-fired Ceramic (LTCC) technology, inserted into the middle of the building material through small cut roughly equal to the thickness of mortar joints in existing buildings or into the plaster during the construction process [5,41].

While this method allows for continuous monitoring of the wall, it has limitations. Specifically, measurements are localized to the area where the sensors are placed; additionally, for existing buildings, cutting the wall to introduce sensors is necessary, resulting in a destructive process.

Advantages and disadvantages of non-destructive methods have been outlined in previous studies [37,49]. Notable advantages include the high availability of equipment necessary to perform the test, the ability to record electrical parameters at depths ranging from 5 to 25 cm, and the minimal invasiveness of most electrical methods. On the other

hand, researchers have noted limitations in non-destructive methods, including the requirement to introduce electrodes into the structure of tested materials, for the resistance method, the interference with salts, in dielectric and microwave methods [50], and the ability to provide only a qualitative assessment of the moisture content [30]. Results obtained through electrical methods are expressed as a variation of materials' physical properties, not as specific moisture content values like results given by direct measurements. In order to scale this variation in a percentage of water content, a preliminary diagnosis of construction materials is necessary. Alternatively, values recorded in the areas affected by humidity phenomena must be compared to values recorded in the areas in a healthy status.

With the aim to overcome both the limits of non-destructive methods employing electrical resistivity or capacitive sensors [51] and infrared thermography [52], some researchers have developed diagnosis approaches applying ground penetrating radar techniques (GPR) at the architectural scale [32,46,50,51,53]. As observed in other non-invasive methods, the validation of the GPR method for measuring moisture contents in masonries closely depends on the type of material investigated.

For any non-destructive methods, it is crucial to clarify the test objective before selecting the appropriate technique. Considering errors associated with the capability of some methods to detect only limited wall thicknesses, as well as the interference of salts, which varies depending on the height of their crystallization on the evaporative surface, is essential to achieve a thorough interpretation of recorded data [31].

1.4. Aim of the research developed

In this study, electrical tests were conducted to overcome some limitations identified in previously analysed methods and introduce an innovative way to establish the preservation level of traditional masonries. The paper shows the results of a research carried out at the Laboratory of Building Engineering of the University of Naples Federico II. The study wants to validate the use of non-destructive electrical measurements, recorded through a coplanar face electric condenser, for estimating the moisture content in traditional masonries. Subsequently, this information is utilised to determine the necessary interventions for walls' regular maintenance, conservation, consolidation or replacement. The results have been obtained by comparing known moisture contents and electrical measurements recorded in the laboratory on samples of Neapolitan Yellow Tuff, and correlating them with corresponding decay levels identified in the literature review (refer to Tables 1 and 2). The methodology can be easily applied to any building material regardless the presence of salts, as it does not aim for precise estimation of moisture content but rather focuses on performance ranges functional for application in the field of recovery projects.

2. Materials and methods

2.1. Building material analyzed

The methodological approach of this survey bases on a comparative analysis between direct measurements of moisture contents in traditional building materials, carried out using the weight method (UNI 11,085 [28]), and the indirect measurements of the electrical properties variation recorded on the same samples in different saturation levels.

Tests were conducted on Neapolitan Yellow Tuff, a soft and workable natural rock historically used in the Neapolitan Built Heritage due to its good resistance, in relation to the specific weight, and for the low cost. This material is the product of the third cycle of volcanic activity of Campi Flegrei, the second for importance in the Campania region [6,7]. Before the investigation process, a prior characterization of physical properties of this material was performed. Using the Equation (1), the percentage of physiological moisture $C_{w,p}$ was determined, representing

the moisture content of the material in thermodynamic equilibrium with the environment under standard conditions of temperature and humidity [54]:

$$C_{w,p} = \frac{(M_f - M_d)}{M_d} \times 100 \quad (1)$$

Where M_f is the mass of the sample in thermodynamic equilibrium with the environment, and M_d is the mass of sample after drying process carried out through the application of gravimetric test. This rate corresponds to the amount of water contained in the material in healthy working conditions. Laboratory tests established that the physiological moisture $C_{w,p}$ of Neapolitan Yellow Tuff varies from 4.98 % to 5.26 %.

For the test, two blocks with dimensions 20 cm x 20 cm x 15 cm, labelled A and B, were used. These dimensions were determined based on the limitations of the coplanar face electric condenser used for electrical measurements, as described in paragraph 2.2.

2.2. Electrical measurement instrument used

The electrical measurements were performed using the IDROSCAN® probe, a coplanar face electric condenser measuring 17 cm x 14 cm x 3 cm, developed by the Italian Company Leonardo Solutions srl, an industrial partner in the research conducted at the University of Naples Federico II. A schematic image of IDROSCAN® probe is presented in Fig. 1. The probe consists of two coplanar electrodes forming a capacitance meter obtained by printing copper on Teflon, a non-hygroscopic material that is sufficiently slippery in contact with the wall surface. The operating principle of IDROSCAN® is protected by industrial patents owned by Leonardo Solutions Srl: UIBM No. 0,001,391,106 and EPO n°2157491.

The device operates on a surface area of 10 cm x 10 cm, but measurements have been recorded on Neapolitan yellow tuff blocks with faces of 20 cm x 20 cm to minimise boundary effects. The measurements were taken by simply touching the inspected surface. The value of the electrical parameter recorded varies according to the moisture content inside the material. The device operates at depths ranging from 5 cm to 10 cm. Considering that the distribution of moisture content inside the block is not uniform in intermediate saturation stages, a thickness of blocks equal to 15 cm was chosen, and the measurements taken on both faces were averaged. The electronic circuit produces a continuous voltage whose capacity varies according to the variation of the moisture

content in the solid medium crossed by the electric impulse with semi elliptical waves. Depending on the degree of saturation of building materials, the electrical response varies. Data recorded are output as numeric values expressed in Idroscan units (u.i.). For the purposes of this experiment, investigating the correspondence between Idroscan units and electrical parameters expressed in the international reference system was considered not significant, as the analysis conducted is comparative.

2.3. Methodological approach

The research focuses on the possibility to measure the variation of electrical parameters of wet and dry walls in order to identify residual performance of building materials. The data recorded enable the definition of the preservation level of existing walls, allowing the determination of appropriate recovery interventions. For this scope, the design of the measuring probe and the conversion of the electrical measurement into an international reference system are not significant factors. Two comparative approaches can be applied to determine preservation levels of historic masonries. In cases where the laboratory characterization of building material is possible, a scale of electrical measurements on the material conditioned with known saturation contents can be established. By comparing this scale with on-site measurements, the preservation level can be determined. On the contrary, when the characterization of building materials cannot be conducted, the preservation level can be established by comparing values obtained from non-invasive tests on dry areas, which the non-invasive analyses show to be in thermo-hygrometric equilibrium with the environment, with those recorded on the wet areas exhibiting superficial anomalies. Both the approaches involve comparing values recorded under the same conditions, thus overcoming limitations caused by salts interference and the instrument's adhesion quality to the detected surface.

In this experimental survey, the first approach was applied. Two blocks have been tested using the gravimetric method, with saturation achieved through a complete immersion in the water an subsequent air evaporation. The samples were weighted at different stages to determine the moisture content, and simultaneously tested with the IDROSCAN® probe.

The workflow of the experimental methodology followed is represented in Fig. 2 (Fig. 2).

The test followed this phases:

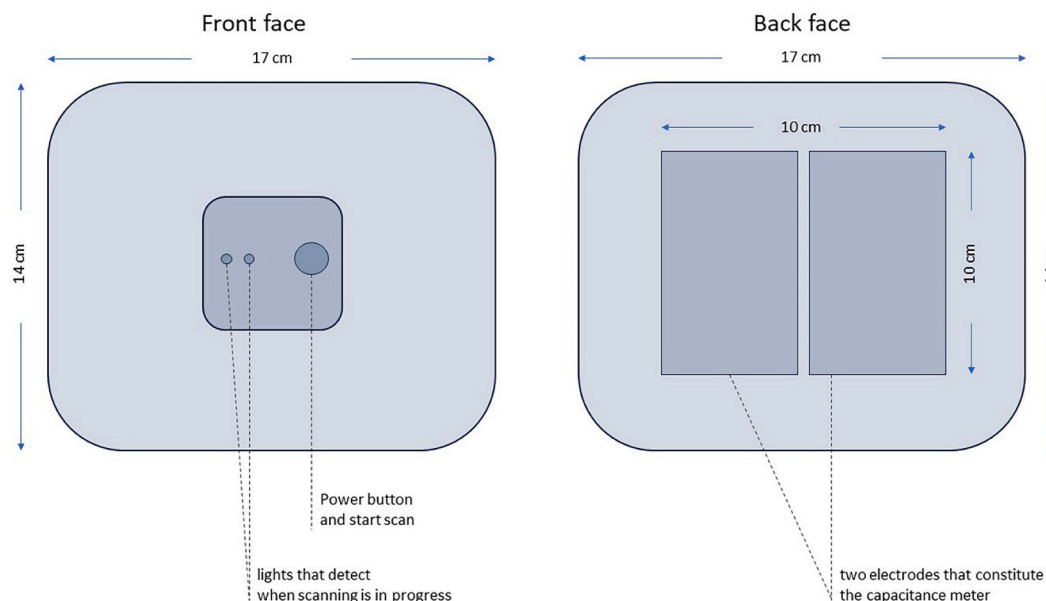


Fig. 1. IDROSCAN® probe scheme.

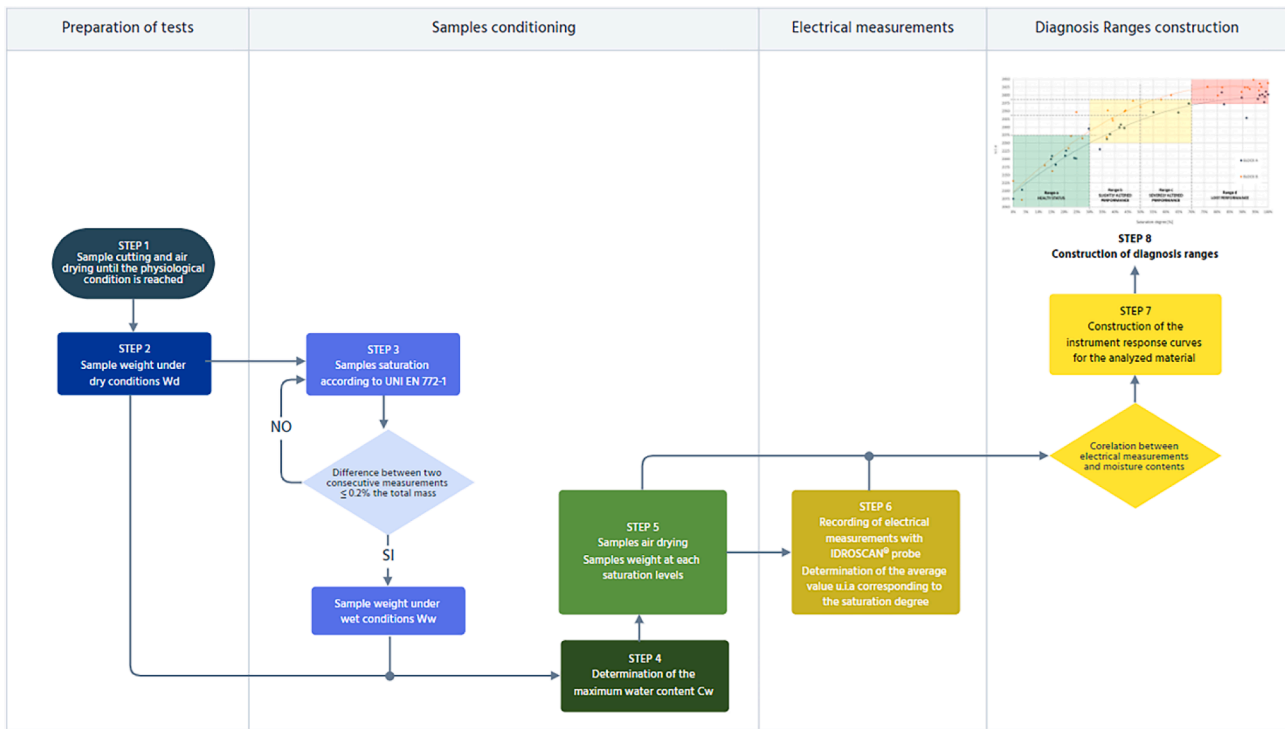


Fig. 2. Methodological workflow.

Step 1: after cutting, samples were dried in the open air until reaching the physiological condition. This condition was considered achieved when the mass of the samples exposed to air stabilized, indicating a difference less than 0.2 % the total mass between two successive weights [3];

Step 2: blocks A and B were weighted in dry conditions, determining the dry weight W_d , which corresponds to the physiological condition (Fig. 3.a);

Step 3: blocks A and B were saturated according to UNI EN 772-1 [3] (Fig. 3.b). Weights were recorded until the difference between two consecutive measurements was less than 0.2 % the total mass, determining the wet weight W_w (Fig. 3.c);

Step 4: applying Equation (2), the maximum water content C_w was determined for both blocks.

$$C_w = \frac{(W_w - W_d)}{W_d} \times 100 \quad (2)$$

Results are summarized in Table 3.

Step 5: blocks were positioned in the open air, in a well-ventilated environment and shielded from direct solar radiation. During the evaporative phase, weights were recorded, and the corresponding saturation level was determined, as presented in Table 4. To facilitate comparison, moisture contents were considered in relation to the blocks' volumes C_w/V .

Step 6: at each weighting stage, electrical measurements with

IDROSCAN® probe were recorded (Fig. 4). Both faces of the two blocks were tested, recording 4 values on each side, making a total of 480 measurements. The data, expressed in Idroscon units u.i., were averaged to determine the average value $u.i.a$ corresponding to the saturation degree.

Results are presented in Table 5 for block A and Table 6 for block B.

In the tables: W is the recorded weight; C_w/V is the moisture content per unit of volume; $u.i.n$ represents the values of electrical measurements recorded on the upper face, $u.i.n$ represents the values of electrical measurements recorded on the back face; $u.i.a$ represents the average of recorded values; Sd is the standard deviation.

Step 7: electrical measurements recorded through the IDROSCAN® probe were correlated with moisture contents determined through the gravimetric method, ranging from the wet to the dry condition. Trend curves representing the instrument response curves of the IDROSCAN® probe for Neapolitan Yellow Tuff were identified for each data group (Fig. 5).

Step 8: values describing the decay of mechanical and thermal performance of building materials affected by humidity phenomena were summarized from the literature review (Tables 1 and 2). By intersecting these data with the instrument response curves, four diagnosis ranges were determined, representing the preservation status of traditional masonries built with Neapolitan Yellow Tuff (Fig. 6).

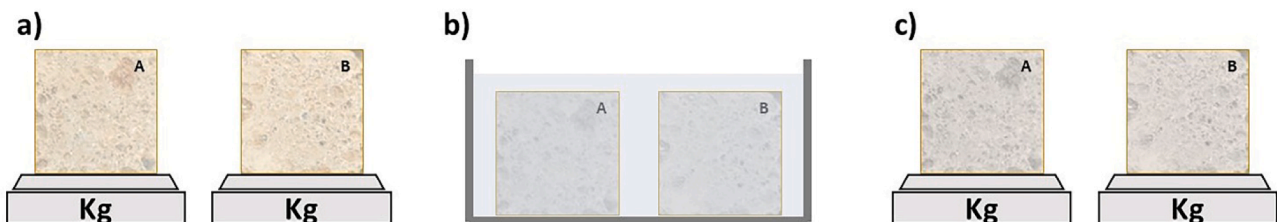


Fig. 3. Steps for samples conditioning and determination of dried weight W_d and wet weight W_w .

Table 3
Dimensions and parameters of tested blocks.

	front side dimensions			back side dimensions			height[cm]	Volume [cm ³]	Weights		Maximum Water content
	side a[cm]	side b[cm]	Area [cm ²]	side a'[cm]	side b'[cm]	Area' [cm ²]			Wd [gr]	Ww[gr]	Cw[gr]
A	19,8	20,1	398,0	19,7	20,0	394,0	15,0	5939,9	8212,0	6103,7	2108,3
B	20,3	19,9	404,0	20,2	20,0	404,0	14,8	5979,0	8160,5	6157,8	2002,7

Table 4
Weights and water contents C_w recorded during the evaporation phase.

Number of measurement	Block A			Block B		
	W [gr]	Cw/V [gr/dm ³]	Cw [%]	W [gr]	Cw/V [gr/dm ³]	Cw [%]
30	6124,00	0,00	0,0%	6172,80	0,00	0,0%
29	6196,60	12,22	3,4%	6240,40	11,31	3,4%
28	6436,50	52,61	14,8%	6422,60	41,78	12,5%
27	6445,00	54,04	15,2%	6481,70	51,66	15,4%
26	6474,90	59,08	16,6%	6608,10	72,81	21,7%
25	6554,10	72,41	20,4%	6627,90	76,12	22,7%
24	6561,10	73,59	20,7%	6668,80	82,96	24,8%
23	6629,00	85,02	24,0%	6717,90	91,17	27,2%
22	6644,20	87,58	24,7%	6907,30	122,85	36,7%
21	6750,60	105,49	29,7%	6916,70	124,42	37,1%
20	6840,90	120,69	34,0%	6951,80	130,29	38,9%
19	6898,70	130,42	36,7%	6955,30	130,88	39,1%
18	6925,30	134,90	38,0%	7047,40	146,28	43,7%
17	7001,20	147,68	41,6%	7057,30	147,93	44,2%
16	7013,80	149,80	42,2%	7114,50	157,50	47,0%
15	7043,40	154,79	43,6%	7174,42	167,52	50,0%
14	7283,70	195,24	55,0%	7336,40	194,62	58,1%
13	7491,50	230,22	64,9%	7414,50	207,68	62,0%
12	7576,60	244,55	68,9%	7700,60	255,53	76,3%
11	7850,20	290,61	81,9%	7780,80	268,94	80,3%
10	7869,20	293,81	82,8%	7815,70	274,78	82,0%
9	8014,90	318,34	89,7%	7968,20	300,29	89,6%
8	8053,70	324,87	91,5%	7992,80	304,40	90,9%
7	8147,50	340,67	96,0%	8015,60	308,21	92,0%
6	8162,90	343,26	96,7%	8031,50	310,87	92,8%
5	8185,00	346,98	97,8%	8060,60	315,74	94,3%
4	8200,00	349,50	98,5%	8104,50	323,08	96,5%
3	8205,50	350,43	98,7%	8111,50	324,25	96,8%
2	8215,30	352,08	99,2%	8122,80	326,14	97,4%
1	8232,30	354,94	100,0%	8175,50	334,96	100,0%

3. Results and discussion

Upon analysing the evaporative phases of blocks A and B, distinct behaviours can be discerned due to the measurements being recorded at



Fig. 4. Step 6: electrical measurement phases carried out through IDROSCAN® probe. On the left, the probe positioned on block A; on the right, the probe positioned on block B.

nearly constant hourly interval of about 3 h, as depicted in Fig. 5.

Evaporation from the complete saturated condition ($S = 100\%$) to $S = 90\%$ occurs in very slowly times (Fig. 5 range 1). During this phase, only superficial moisture is dispelled. In the range from $S = 90\%$ to $S = 50\%$, the evaporation rate increases due to the temperature and pressure differences between the blocks' surface and the inner layers. This disparity activates a faster evaporative flow (Fig. 5 range 2). In the range from $S = 50\%$ to $S = 15\%$, the evaporation rate decreases again because of the difficulty in disposing of the deeper water contents, which are retained by the closed porosity of samples. (Fig. 5 range 3). In the range from $S = 15\%$ to the dry condition ($S = 0\%$), the evaporation increases once more, reaching a stable mass in equilibrium with the external environment.

Innovative results were obtained by correlating electrical measurements recorded through the IDROSCAN® probe, expressed in u.i. values, with the moisture contents represented in saturation degrees. Fig. 6 represents the Instrumental response curve constructed with Idroscon data presented in Tables 5 and 6 for the specific material of Neapolitan Yellow Tuff. On the y-axis, values represent u.i._a, the average of the values corresponding to the 8 measurements taken for each block, 4 per face, while values the x-axis represents the saturation degree. As the saturation of samples increases, the measured electrical parameter also increases. Three main ranges can be identified describing the electrical behaviour of the building material concerning the saturation degree (Fig. 6). In the first range, from dry conditions ($S = 0\%$) to $S = 30\%$, the correspondence between moisture content and electrical parameter follows an almost linear trend (Fig. 6 range 1). In the second range, from $S = 30\%$ to 70% , a parabolic behaviour is observed. In this range, the variation in the electrical measurement is lower than the corresponding increase in the moisture content (Fig. 6 range 2). In the third range, from $S = 70\%$ to the complete saturated condition ($S = 100\%$), the electrical measurements are very close to each other (Fig. 6 range 3).

Results have been compared with data presented in the literature review (Tab. 1 and Tab. 2) to determine saturation degrees affecting thermal and mechanical performance of building materials. Bibliographic studies had indicated a strong reduction in mechanical performance in semi-saturated ($S = 50\%$) and saturated conditions ($S = 100\%$), as well as in exercise conditions ($S = 20\text{--}30\%$). Table 1

Table 5
Electrical measurements recorded for each side of block A.

Number of measurement	Block A										Sd
	Cw [%]	u.i. 1	u.i. 2	u.i. 3	u.i. 4	u.i.' 1	u.i.' 2	u.i.' 3	u.i.' 4	u.i. a	
30	0,0%	2064	2060	2064	2061	2091	2088	2092	2089	2076	15
29	3,4%	2127	2123	2129	2126	2084	2080	2085	2081	2104	23
28	14,8%	2186	2182	2184	2188	2216	2212	2216	2213	2200	16
27	15,2%	2179	2183	2184	2181	2240	2237	2241	2236	2210	30
26	16,6%	2130	2127	2130	2127	2238	2234	2239	2235	2183	58
25	20,4%	2211	2208	2213	2209	2210	2208	2215	2212	2211	2
24	20,7%	2199	2195	2201	2198	2254	2251	2255	2252	2226	29
23	24,0%	2186	2182	2186	2183	2224	2221	2225	2222	2204	21
22	24,7%	2164	2160	2166	2162	2242	2238	2242	2239	2202	41
21	29,7%	2299	2296	2301	2299	2291	2293	2287	2290	2295	5
20	34,0%	2212	2209	2214	2211	2251	2247	2252	2249	2231	21
19	36,7%	2254	2251	2256	2252	2274	2272	2275	2273	2263	11
18	38,0%	2290	2287	2292	2290	2268	2264	2269	2266	2278	12
17	41,6%	2298	2296	2304	2307	2298	2296	2300	2302	2300	4
16	42,2%	2308	2306	2311	2308	2308	2305	2309	2306	2308	2
15	43,6%	2266	2263	2267	2264	2331	2328	2331	2328	2297	35
14	55,0%	2357	2354	2357	2355	2339	2336	2340	2338	2347	9
13	64,9%	2349	2346	2350	2347	2344	2342	2346	2342	2346	3
12	68,9%	2383	2380	2385	2381	2366	2362	2368	2364	2374	9
11	81,9%	2412	2408	2413	2410	2409	2406	2410	2407	2409	2
10	82,8%	2368	2365	2369	2366	2378	2375	2378	2375	2372	5
9	89,7%	2409	2406	2411	2407	2378	2374	2379	2376	2393	17
8	91,5%	2304	2299	2305	2300	2357	2354	2359	2355	2329	29
7	96,0%	2393	2389	2395	2392	2384	2381	2385	2382	2388	5
6	96,7%	2422	2419	2423	2419	2381	2377	2382	2379	2400	22
5	97,8%	2407	2403	2407	2404	2386	2383	2413	2410	2402	11
4	98,5%	2377	2374	2387	2384	2375	2372	2378	2375	2378	5
3	98,7%	2402	2399	2406	2403	2390	2387	2390	2387	2396	8
2	99,2%	2434	2433	2444	2441	2384	2381	2385	2382	2411	30
1	100,0%	2423	2421	2434	2430	2377	2374	2378	2375	2402	28

Table 6
Electrical measurements recorded for each side of block B.

Number of measurement	Block B										Sd
	Cw [%]	u.i. 1	u.i. 2	u.i. 3	u.i. 4	u.i.' 1	u.i.' 2	u.i.' 3	u.i.' 4	u.i. a	
30	0,0%	2164	2160	2164	2161	2101	2097	2102	2098	2131	34
29	3,4%	2089	2084	2089	2086	2057	2054	2059	2055	2072	17
28	12,5%	2238	2234	2236	2232	2129	2126	2130	2126	2181	57
27	15,4%	2199	2196	2198	2201	2128	2124	2128	2124	2162	39
26	21,7%	2261	2257	2261	2259	2209	2206	2210	2208	2234	27
25	22,7%	2304	2301	2305	2302	2241	2237	2243	2239	2272	34
24	24,8%	2342	2339	2339	2335	2327	2324	2327	2325	2347	31
23	27,2%	2337	2335	2339	2336	2194	2191	2196	2193	2265	77
22	36,7%	2305	2302	2313	2309	2232	2229	2234	2230	2269	41
21	37,1%	2422	2418	2423	2420	2282	2279	2287	2284	2352	74
20	38,9%	2390	2388	2391	2388	2264	2261	2269	2265	2327	67
19	39,1%	2395	2392	2397	2395	2247	2243	2248	2245	2320	80
18	43,7%	2424	2420	2423	2420	2275	2273	2278	2276	2349	78
17	44,2%	2430	2426	2430	2427	2276	2272	2278	2276	2352	82
16	47,0%	2457	2453	2456	2453	2311	2308	2312	2309	2382	77
15	50,0%	2416	2412	2419	2413	2312	2308	2314	2311	2363	56
14	58,1%	2446	2442	2447	2443	2328	2324	2330	2327	2386	63
13	62,0%	2450	2446	2450	2446	2351	2348	2357	2355	2400	51
12	76,3%	2481	2476	2479	2476	2376	2372	2376	2373	2426	55
11	80,3%	2453	2450	2456	2452	2345	2343	2349	2346	2399	57
10	82,0%	2469	2464	2468	2464	2381	2378	2384	2381	2424	46
9	89,6%	2446	2442	2446	2442	2377	2373	2379	2376	2410	36
8	90,9%	2407	2468	2474	2470	2391	2388	2399	2395	2424	39
7	92,0%	2457	2453	2457	2453	2395	2391	2395	2392	2424	33
6	92,8%	2460	2457	2453	2457	2376	2373	2391	2388	2419	40
5	94,3%	2469	2468	2476	2473	2425	2421	2427	2423	2448	26
4	96,5%	2420	2417	2424	2421	2408	2405	2413	2409	2415	7
3	96,8%	2422	2418	2421	2418	2453	2450	2456	2452	2436	18
2	97,4%	2427	2470	2473	2470	2393	2390	2395	2392	2426	39
1	100,0%	2434	2430	2440	2436	2439	2437	2447	2444	2438	5

demonstrates the different behaviours of various materials in terms of reduction of compressive strengths due to the saturation degree. Selecting a single reference value or an average of values could impact

the validity of data interpretation, crucial for this survey's purposes. In order to establish a correspondence between the instrumental response curve of the electrical probe used and the mechanical performance of the

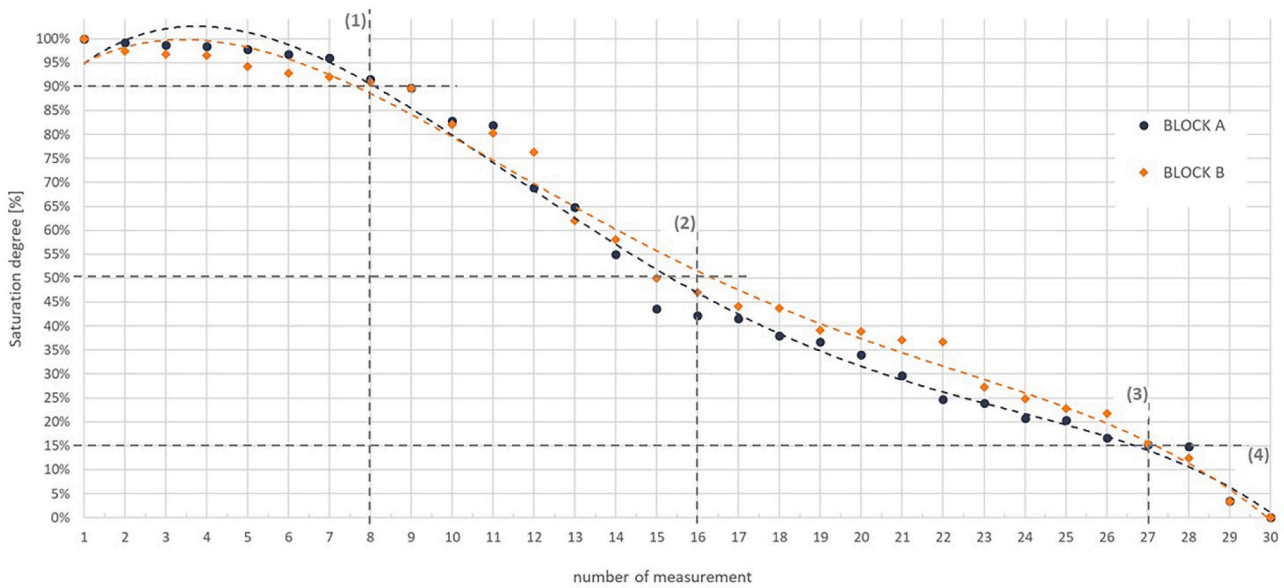


Fig. 5. Evaporative phases of Blocks A and B.

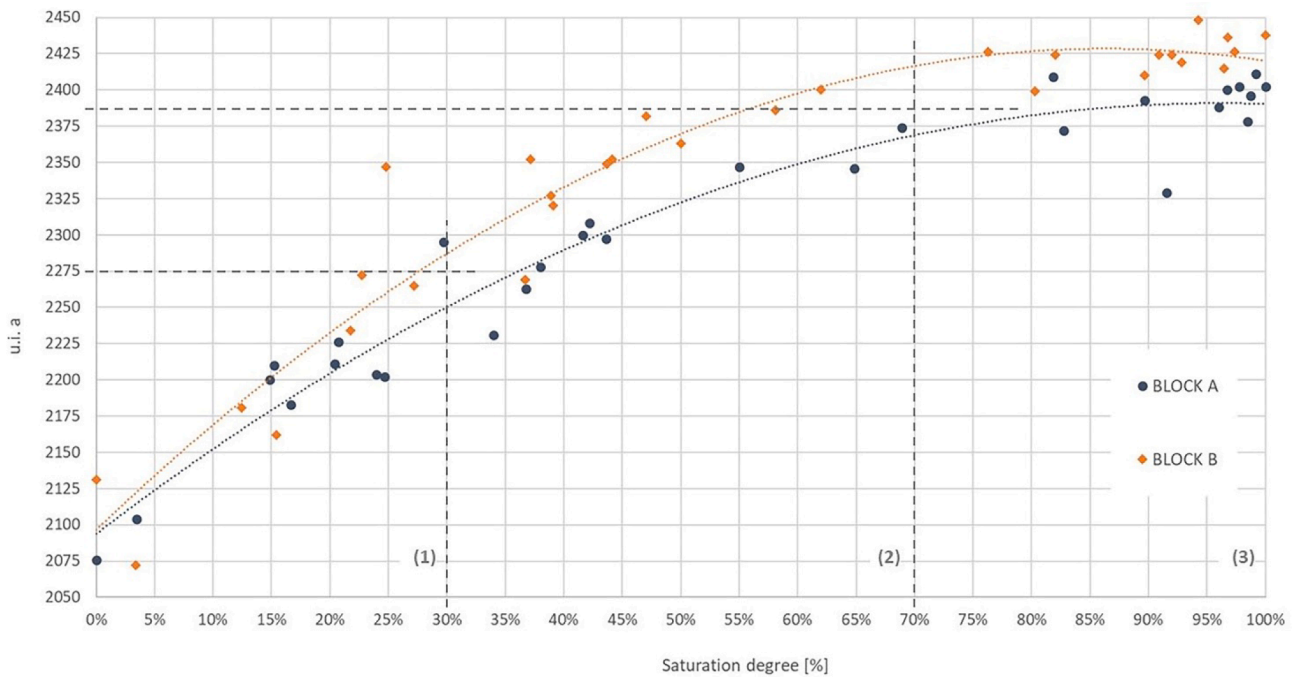


Fig. 6. Instrumental response curve built with Idroscan data for blocks A (blue) and B (orange). (For interpretation of the references to colour in this figure legend, the reader is referred to the web version of this article.)

analysed material, only references related to Yellow Tuff testing were considered [6,7]. Depending on the experience, the saturation degree $S = 20\text{--}30\%$ can be considered the limit value to assess a masonry in healthy conditions (Fig. 7 range a). In semi-saturated conditions ($S = 50\%$), the average decrease of compressive strengths is approximately 30%. In this scenario, a large range of preservation levels includes both slightly altered performance and severely altered performance. This range requires a detailed diagnosis phase to determine the recovery intervention, ranging from light to the heavy interventions (Fig. 7 ranges b and c). In saturated conditions ($S = 100\%$), the average decrease in compressive strengths exceeds 45%. In this scenario, construction materials lose mechanical performance required for structural standards. The design of recovery interventions must consider either a partial

replacement of degraded masonries or, when not allowed due to the building's cultural value, a strong consolidation (Fig. 7 range d).

The same analysis was conducted using bibliographic data concerning the decrease in thermal performance of building materials due to moisture contents [Tab. 2]. Specific reference was made to data elaborated in the previous stage of this research, enabling a comparison between saturation degrees and the thermal conductivity of porous materials [9]. In Fig. 8, several thermal performance ranges are highlighted. The saturation degree $S = 20\text{--}30\%$ is confirmed as the limit value to assess a masonry in healthy conditions (Fig. 8 range a). Thermal behaviour recorded on masonries by other researchers [21,22] demonstrates that, in this range, the decrease of walls' thermal behaviour may be higher. This observation emphasizes the impact of external and

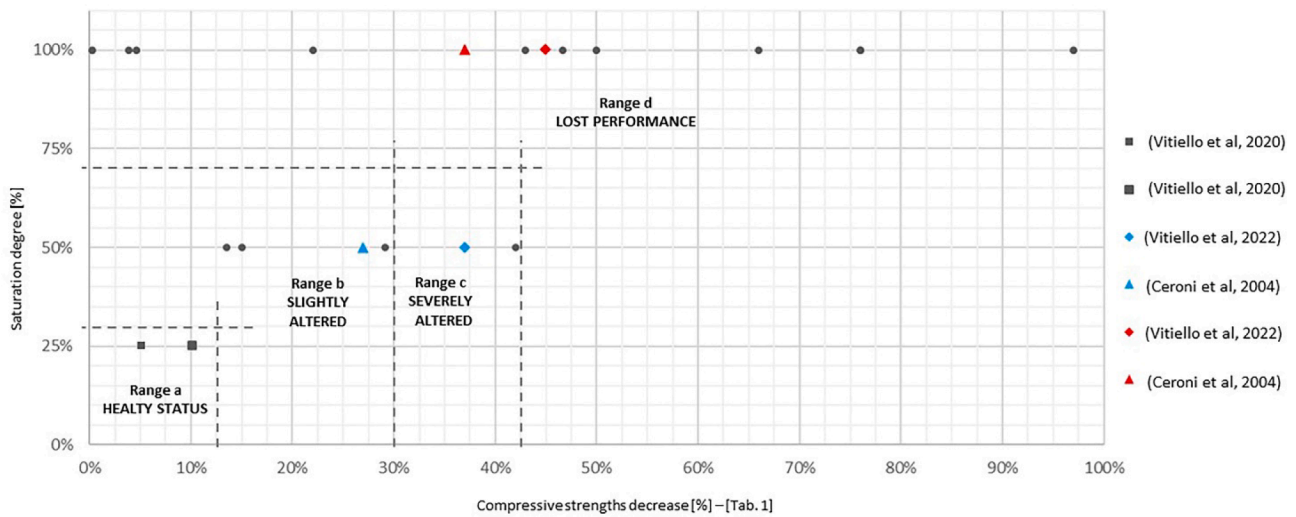


Fig. 7. Compressive performance decrease related to saturation degrees.

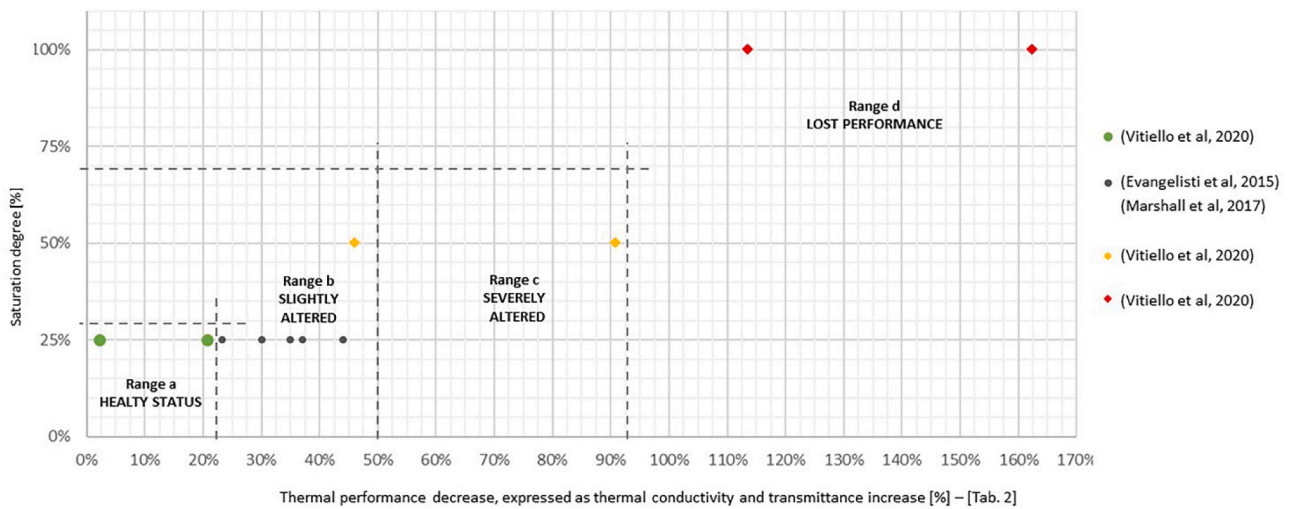


Fig. 8. Thermal performance decrease related to saturation degrees.

internal finishing layers on the overall transmittance of the building envelope’s technical elements. External layers are affected by rainfall, while internal layers are subjected to condensation phenomena. In this study, the focus is on establishing a relationship between thermal and mechanical parameters and electrical measurements specific for the material. Therefore, references related to data recorded on the entire technical element are not taken into account. In semi-saturated conditions ($S = 50\%$), thermal properties significantly increase. In this scenario, diagnosis phase must include both direct and indirect measurements to determine the causes of the phenomenon and assess the masonry preservation levels. The design phase will promote lighter maintenance interventions, by enhancing the evaporation of moisture by means of forced ventilation or using macro-porous plasters, if values stay in the range of slightly altered performance (Fig. 8 range b). For higher values (Fig. 8 range c), more substantial conservation interventions should be promoted to arrest the water absorption and to eliminate moisture contents. Priority should be given to non-invasive techniques [1]. In saturated conditions ($S = 100\%$), thermal performance decrease to values unsuitable for built environments. Considering the significant impact on mechanical strengths, the partial replacement of degraded masonries is confirmed as a viable solution (Fig. 8 range d).

In all the analysed scenarios, recorded values illustrate the

considerable disparity between calculated thermal performance and the real behaviour of walls in exercise conditions. This type of diagnosis demonstrates the importance to understand the state of preservation of walls before designing any recovery project. Without a thorough diagnosis, certain humidity phenomena may be underestimated, leading to surface-level treatments, while as demonstrated, they could denounce the need to intervene even with consolidation actions.

By intersecting the performance ranges showed in Figs. 7 and 8 with the instrumental response curve generated using the IDROSCAN® probe for the analysed material, showed in Fig. 6, four diagnosis ranges regarding the preservation of Neapolitan Yellow Tuff’s masonries are identified: masonries in healthy conditions, with slightly altered performance (Fig. 9 range a), masonries displaying slightly altered performance, warranting moderate interventions (Fig. 9 range b), masonries displaying severely altered performance, requiring substantial conservation efforts (Fig. 9 range c) or masonries with complete loss of performance, necessitating extensive interventions or replacement (Fig. 9 range d).

A non-destructive diagnosis of existing walls made with this natural stone can be conducted through the following simple phases: touching the wall surface with the IDROSCAN® probe; recording electrical values obtained from the probe; entering in the instrumental response curve

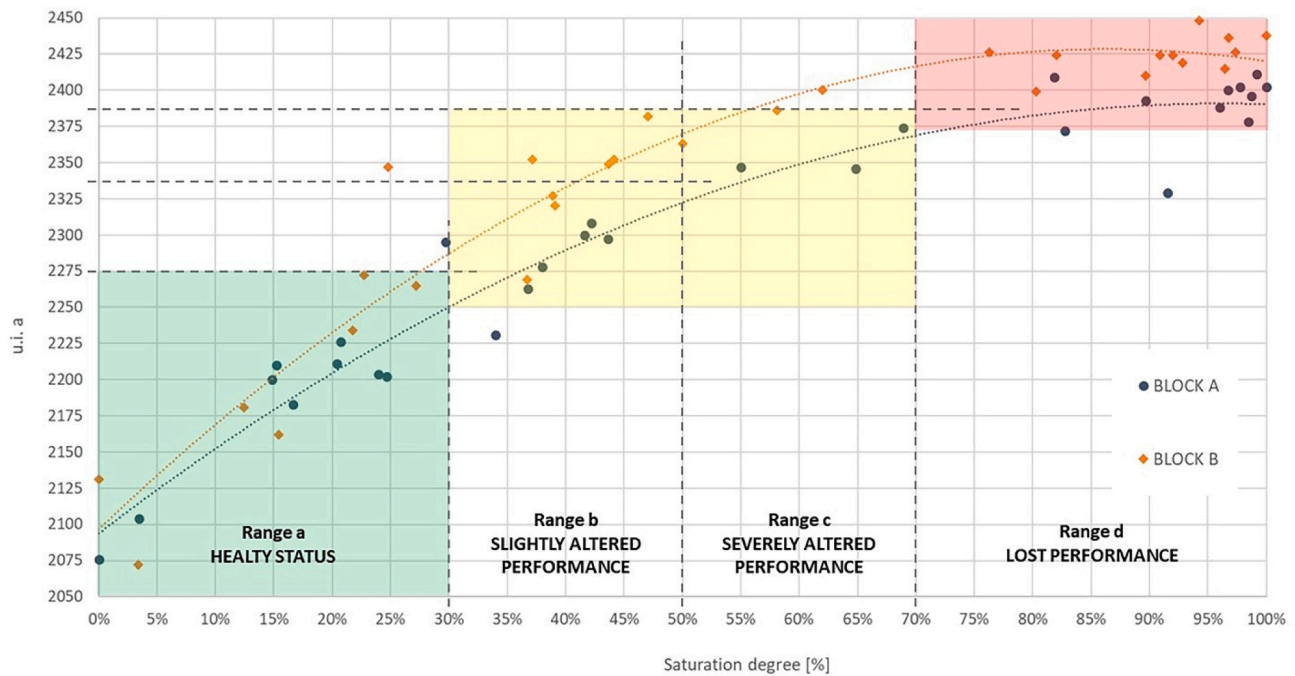


Fig. 9. Idroscan diagnosis ranges for Neapolitan Yellow Tuff. (For interpretation of the references to colour in this figure legend, the reader is referred to the web version of this article.)

with the recorded value u.i.; determining the corresponding diagnosis range; defining the range of suggested recovery interventions; programming monitoring and final check phases.

Monitoring the effectiveness of the intervention can be conducted by analysing the variation in electrical values from the initial to the final phase, once moisture contents have been disposed of. Successful intervention is indicated when the preservation status of masonry portions previously affected by humidity phenomena records electrical values that are close to those recorded on portions of the same masonry or building that were not affected by these issues.

4. Conclusions

Results obtained by this research demonstrates the applicability of non-destructive diagnosis techniques in determining the preservation level of existing masonries. The use of electrical measurements in a comparative analysis exceeds challenges related to the precise correspondence between electrical data detected and the moisture content. By changing the scope of the test, and leading it back to a comparative analysis, the sensitivity of instruments used, the interference with salts and the conversion of Idroscan units in the International Reference System, can be disregarded.

The potential of this research lies in its ability to intersect bibliographic data with empirical data, leading to the development of an operational and applicable non-invasive diagnostic methodology suitable for different contexts. Diagnosis ranges built for Neapolitan Yellow Tuff with the IDROSCAN® probe, can be used in practical applications in order to: detect preservation levels of traditional Neapolitan masonries; define the design phases for the recovery of wet walls; monitor the effectiveness of the intervention chosen during the time; certify the final check.

This approach fills a regulatory gap concerning to the recovery of wet walls, where currently no certificates or tests of the adopted techniques are mandatory. This often leads to interventions on the Built Heritage based on empirical knowledge rather than scientific rigour.

Compared to quantitative methods, the proposed approach provides a measurement through non-invasive analysis of the wet content.

Compared to qualitative methods, it avoids many interference factors that could alter the diagnosis or necessitates further data processing for accurate interpretation. These aspects make the method valuable for the non-invasive monitoring of the walls subjected to a recovery intervention and the validation of performance and techniques employed. Its non-invasive nature makes it especially suitable for Cultural Heritage applications.

However, a potential limitation might arise if the established curve for the Neapolitan Yellow Tuff proves not to be universally applicable to different traditional construction materials. In such cases, specific instrumental response curves might to be developed for each distinct material. Future research developments could explore the possibility of creating a database comprising instrument response curves for common traditional construction materials such as bricks, sandstones or other types of Tuff (Yellow but not chaotic, grey, green etc.).

CRediT authorship contribution statement

Veronica Vitiello: Conceptualization, Data curation, Investigation, Methodology, Visualization, Writing – original draft, Writing – review & editing. **Roberto Castelluccio:** Supervision, Funding acquisition, Conceptualization, Writing – original draft. **Paola Villoria Sáez:** Writing – review & editing, Investigation.

Declaration of Competing Interest

The authors declare the following financial interests/personal relationships which may be considered as potential competing interests: Veronica Vitiello reports financial support was provided by Government of Italy Ministry of Education University and Research. Veronica Vitiello reports a relationship with Government of Italy Ministry of Education University and Research that includes.

Data availability

Data will be made available on request.

Acknowledgement

The experimental laboratory research presented in this contribution was developed thanks to the support of some project partners who authors would like to thank. Leonardo Solutions srl, the owner of patents for industrial invention of the IDROSCAN® probe, which participates in the project as an industrial partner and has made available the technology and tools for the execution of electrical tests. Professor Fabio Iucolano of the University of Naples Federico II, who provided support for the physical properties characterization of the analysed material and the measurement of the physiological moisture at the Materials Engineering Laboratory of the University.

Fundings

The research presented in this contribution is financed by Government of Italy Ministry of Education University and Research to the Department of Civil, Building and Environmental Engineering (D.I.C.E.A.) of the University of Naples Federico II through PON R&I 2014-2020 - Axis IV "Education and research for recovery - REACT-EU", Action IV.4 - "Research contracts on innovation issues". The funding source has no involvement on the decision to submit the article for publication.

References

- V. Vitiello e R. Castelluccio, Il risanamento delle murature affette da umidità da risalita capillare. Il metodo CNT, Napoli: Luciano Editore, 2019.
- J.-L. Jaskowska and E. Przesmycka, "Semi-Destructive and Non-Destructive Tests of Timber," *Materials (Basel)*, vol. 14, no. 1, pp. 1–22, 2020, [Online]. Available: doi.org/10.3390/ma14010096.
- UNI, 772-11. *Metodi di prova per elementi per muratura – parte 11*, 2011.
- A. Hawkins e B. McConnell, «Sensitivity of sandstone strength and deformability to changes in moisture content,» *Quarterly Journal of Engineering Geology*, vol. 25, n. 2, pp. 115-130, 1992.
- E. Verstrynge, R. Adriaens, J. Elsen, K. Van Balen, Multi-scale analysis on the influence of moisture on the mechanical behavior of ferruginous sandstone, *Constr. Build. Mater.* 54 (2014) 78–90, <https://doi.org/10.1016/j.conbuildmat.2013.12.024>.
- R. Ceroni, M. Pece, G. Manfredi e G. Marcarì, «Analisi e caratterizzazione meccanica di murature di tufo,» in *15° Congresso C.T.E.*, Bari, 2004.
- V. Vitiello, R. Castelluccio, and M. Ramondini, *Conservation of Cultural Heritage. Evaluation of Archaeological Digs Effect on the Degradation of the Structures Found*, vol. 209 LNCE, no. 1986. Springer International Publishing, 2022. doi: 10.1007/978-3-030-90788-4_57.
- E. Franzoni, C. Gentilini, G. Graziani, S. Bandini, Compressive behaviour of brick masonry triplets in wet and dry conditions, *Constr. Build. Mater.* 82 (2015) 45–52, <https://doi.org/10.1016/j.conbuildmat.2015.02.052>.
- V. Vitiello, R. Castelluccio, M. Del Rio Merino, Experimental research to evaluate the percentage change of thermal and mechanical performances of bricks in historical buildings due to moisture, *Constr. Build. Mater.* 244 (2020), <https://doi.org/10.1016/j.conbuildmat.2020.118107>.
- B. Várshelyi, M. Davarpanah, Influence of water content on the mechanical parameters of the intact rock and rock mass, *Period. Polytech. Civ. Eng.* 62 (4) (2018) 1060–1066, <https://doi.org/10.3311/PPci.12173>.
- P. Colback e B. Wild, «The influence of moisture content on the compressive strength,» in *Proceedings of the 3rd Canadian Rock Mechanics Symposium*, Toronto, Canada, 1965.
- C. Dyke e L. Dobreiner, «Evaluating the strength and deformability of sandstones,» *Quarterly Journal of Engineering Geology and Hydrogeology*, vol. 24, n. 1, p. 123–134, 1991.
- G. Lashkaripour e M. Ghafoori, «The engineering geology of the Tabarak Abad Dam,» *Engineering Geology*, vol. 66, n. 3-4, pp. 233-239, 2002.
- B. Várshelyi, *Some observation regarding the strength and deformability of sandstones in case of dry and saturated conditions*, *Bull. Eng. Geol. Environ.* 62 (3) (2003) 245–249.
- B. Várshelyi, *Statistical analysis of the influence of water content on the strength of the Miocene limestone*, *Rock Mech. Rock Eng.* 38 (1) (2005) 69–76.
- UNI, *EN ISO 6946. Componenti ed elementi per edilizia - Resistenza termica e trasmittanza termica - Metodi di calcolo*, 2018.
- A. Fouquier, S. Robert, F. Suard, L. Stéphan, A. Jay, State of the art in building modelling and energy performances prediction: a review, *Renew. Sustain. Energy Rev.* 23 (2013) 272–288, <https://doi.org/10.1016/j.rser.2013.03.004>.
- P. Baker, U-values and traditional buildings In situ measurements and their comparisons to calculated values D [Online]. Available: Dinburgh, UK (2011) www.historic-scotland.gov.uk/technicalpapers.
- L. Kosmina, Guide to In-situ U-value measurement of walls in existing dwellings In-situ measurement of U-value [Online]. Available: Bre no. September (2016) 1–13 www.bre.co.uk/uvalues.
- S. Doran, Field investigations of the thermal performance of construction elements as built, BRE East Kilbride no. June (2001), <https://doi.org/10.13140/RG.2.1.3397.9042>.
- L. Evangelisti, C. Guattari, P. Gori, R. De Lieto Vollaro, In situ thermal transmittance measurements for investigating differences between wall models and actual building performance, *Sustain.* 7 (8) (2015) 10388–10398, <https://doi.org/10.3390/su70810388>.
- A. Marshall, et al., Domestic building fabric performance: Closing the gap between the in situ measured and modelled performance, *Energy Build.* 150 (2017) 307–317, <https://doi.org/10.1016/j.enbuild.2017.06.028>.
- F. D'Alessandro, G. Baldinelli, F. Bianchi, S. Sambuco, A. Rufini, Experimental assessment of the water content influence on thermo-acoustic performance of building insulation materials, *Constr. Build. Mater.* 158 (2018) 264–274, <https://doi.org/10.1016/j.conbuildmat.2017.10.028>.
- G. Moriconi, M.G. Castellano, M. Collepardi, Mortar deterioration of the masonry walls in historic buildings. a case history: Vanvitelli's Hole in Ancona, Mater. Struct. 27 (7) (1994) 408–414, <https://doi.org/10.1007/BF02473445>.
- L. Binda, C. Colla e M. Forde, «Identification of moisture capillarity in masonry using digital impulse radar,» *Construction and Building Materials*, vol. 8, n. 2, pp. 101-107, 1994.
- R. Castelluccio, V. Vitiello e C. Di Mare, «Il conflitto normativo tra le istanze energetica e della conservazione degli edifici storici non vincolati,» in *Colloqui.AT.e* 2022, Genova, 2022.
- A. Hola, Measuring of the moisture content in brick walls of historical buildings-the overview of methods, *IOP Conf. Ser. Mater. Sci. Eng.* 251 (1) (2017), <https://doi.org/10.1088/1757-899X/251/1/012067>.
- UNI, 11085. *Materiali lapidei naturali ed artificiali. determinazione del contenuto d'acqua: metodo ponderale.*, 2003.
- UNI, 11121. *Beni culturali - Materiali lapidei naturali ed artificiali - Determinazione in campo del contenuto di acqua con il metodo al carburo di calcio*, 2004.
- A. Hola, Ł. Sadowski, A method of the neural identification of the moisture content in brick walls of historic buildings on the basis of non-destructive tests, *Autom. Constr. vol. 106*, no. April (2019), 102850, <https://doi.org/10.1016/j.autcon.2019.102850>.
- A. Hussain, S. Akhtar, Review of non-destructive tests for evaluation of historic masonry and concrete structures, *Arab. J. Sci. Eng.* 42 (3) (2017) 925–940, <https://doi.org/10.1007/s13369-017-2437-y>.
- T. Klewe, C. Strangfeld, S. Kruschwitz, Review of moisture measurements in civil engineering with ground penetrating radar – applied methods and signal features, *Constr. Build. Mater.* 278 (2021), 122250, <https://doi.org/10.1016/j.conbuildmat.2021.122250>.
- B.J. Pease, G.A. Scheffler, H. Janssen, Monitoring moisture movements in building materials using X-ray attenuation: Influence of beam-hardening of polychromatic X-ray photon beams, *Constr. Build. Mater.* 36 (2012) 419–429, <https://doi.org/10.1016/j.conbuildmat.2012.04.126>.
- W. Wang, K. Zhao, P. Zhang, J. Bao, S. Xue, Application of three self-developed ECT sensors for monitoring the moisture content in sand and mortar, *Constr. Build. Mater.* 267 (2021), 121008, <https://doi.org/10.1016/j.conbuildmat.2020.121008>.
- S. Rubene, M. Vilnitis, Application of electrical impedance spectrometry for measurements of humidity distribution in aerated concrete masonry constructions, *Int. J. Mech.* 9 (1) (2015) 213–219.
- J. Hroudová, M. Sedlmajer, J. Pařílková, J. Zach, Laboratory testing of developed thermal insulation plasters on pillars built from masonry bricks, *Procedia Eng.* 172 (2017) 377–384, <https://doi.org/10.1016/j.proeng.2017.02.043>.
- J. Galvão, R. Duarte, I. Flores-Colen, J. de Brito, A. Hawreen, Non-destructive mechanical and physical in-situ testing of rendered walls under natural exposure, *Constr. Build. Mater.* 230 (2020), <https://doi.org/10.1016/j.conbuildmat.2019.116838>.
- A. Menezes, M. Glória Gomes, I. Flores-Colen, In-situ assessment of physical performance and degradation analysis of rendering walls, *Constr. Build. Mater.* 75 (2015) 283–292, <https://doi.org/10.1016/j.conbuildmat.2014.11.039>.
- Z. Pavlík, J. Mihulka, L. Fiala, R. Černý, Application of time-domain reflectometry for measurement of moisture profiles in a drying experiment, *Int. J. Thermophys.* 33 (8–9) (2012) 1661–1673, <https://doi.org/10.1007/s10765-011-1020-0>.
- L. Alwis, T. Sun, K.T.V. Grattan, Optical fibre-based sensor technology for humidity and moisture measurement: Review of recent progress, *Meas. J. Int. Meas. Confed.* 46 (10) (2013) 4052–4074, <https://doi.org/10.1016/j.measurement.2013.07.030>.
- M. Maksimović, et al., Application of a LTCC sensor for measuring moisture content of building materials, *Constr. Build. Mater.* 26 (1) (2012) 327–333, <https://doi.org/10.1016/j.conbuildmat.2011.06.029>.
- J. Hola, Z. Matkowski, K. Schabowicz, J. Sikora, S. Wojtczak, "New method of investigation of rising damp in brick walls by means of impedance tomography", 17th World Conf [Online]. Available: Nondestruct. Test. no. January (2008) 8 <http://www.ndt.net/article/wcndt2008/papers/463.pdf>.
- N. Ludwig, E. Rosina, A. Sansonetti, Evaluation and monitoring of water diffusion into stone porous materials by means of innovative IR thermography techniques, *Meas. J. Int. Meas. Confed.* 118 (July) (2018) 348–353, <https://doi.org/10.1016/j.measurement.2017.09.002>.
- E. Barreira, R.M.S.F. Almeida, J.M.P.Q. Delgado, Infrared thermography for assessing moisture related phenomena in building components, *Constr. Build. Mater.* 110 (2016) 251–269, <https://doi.org/10.1016/j.conbuildmat.2016.02.026>.
- J. Szczotka, Non-invasive methods in diagnosis of wall dampness degree in sacral buildings, *Diagnostyka* 19 (2) (2018) 63–69, <https://doi.org/10.29354/diag/86514>.
- G.P. Cetrangolo, L.D. Domenech, G. Moltini, A.A. Morquío, Determination of moisture content in ceramic brick walls using ground penetration radar,

- J. Nondestruct. Eval. 36 (1) (2017) 1–11, <https://doi.org/10.1007/s10921-016-0390-4>.
- [47] K.G. Ong, C.A. Grimes, C.L. Robbins, R.S. Singh, Design and application of a wireless, passive, resonant-circuit environmental monitoring sensor, *Sensors Actuators, A Phys.* 93 (1) (2001) 33–43, [https://doi.org/10.1016/S0924-4247\(01\)00624-0](https://doi.org/10.1016/S0924-4247(01)00624-0).
- [48] Z. You, J. Mills-Beale, B.D. Pereles, K.G. Ong, A wireless, passive embedded sensor for real-time monitoring of water content in civil engineering materials, *IEEE Sens. J.* 8 (12) (2008) 2053–2058, <https://doi.org/10.1109/JSEN.2008.2007681>.
- [49] R. Cacciotti, J. Valach, B. Wolf, Innovative and easy-to-implement moisture monitoring system for brick units, *Constr. Build. Mater.* 186 (2018) 598–614, <https://doi.org/10.1016/j.conbuildmat.2018.07.125>.
- [50] G.M. Carlomagno, R. Di Maio, M. Fedi, C. Meola, Integration of infrared thermography and high-frequency electromagnetic methods in archaeological surveys, *J. Geophys. Eng.* 8 (3) (2011) pp, <https://doi.org/10.1088/1742-2132/8/3/S09>.
- [51] Y. El Masri, T. Rakha, A scoping review of non-destructive testing (NDT) techniques in building performance diagnostic inspections, *Constr. Build. Mater.* 265 (2020), 120542, <https://doi.org/10.1016/j.conbuildmat.2020.120542>.
- [52] V. Malhotra e N. Carino, *Handbook on Nondestructive Testing of Concrete*, 2nd Edition a cura di, Boca Raton: CRC Press, 2003.
- [53] S. Laurens, J. Balayssac, J. Rhazi, G. Klysz e G. Arliguie, «Non-destructive evaluation of concrete moisture by GPR: Experimental study and direct modeling,» *Materials and Structures*, vol. 38, n. 19, pp. 827-832, 2005.
- [54] G. Alfano, F. d'Ambrosio e G. Riccio, *L'umidità ascendente*, Napoli: de Costanzo Editori, 1996.